
1

INORGANIC CHEMISTRY ESSENTIALS

1.1 INTRODUCTION

Bioinorganic chemistry involves the study of metal species in biological systems. As an introduction to basic inorganic chemistry needed for understanding bioinorganic topics, this chapter will discuss the essential chemical elements, the occurrences and purposes of metal centers in biological species, the geometries of ligand fields surrounding these metal centers, and the ionic states preferred by the metals. Important considerations include equilibria between metal centers and their ligands and a basic understanding of the kinetics of biological metal–ligand systems. The occurrence of organometallic complexes and clusters in metalloproteins will be discussed briefly, and an introduction to electron transfer in coordination complexes will be presented. Because the metal centers under consideration are found in a biochemical milieu, basic biochemical concepts, including a discussion of proteins and nucleic acids, are presented in Chapter 2.

1.2 ESSENTIAL CHEMICAL ELEMENTS

Chemical elements essential to life forms can be broken down into four major categories: (1) bulk elements (H, C, N, O, P, S); (2) macrominerals and ions (Na, K, Mg, Ca, Cl, PO_4^{3-} , SO_4^{2-}); (3) trace elements (Fe, Zn, Cu); and (4) ultratrace elements, comprised of nonmetals (F, I, Se, Si, As, B) and metals (Mn, Mo, Co, Cr, V, Ni, Cd, Sn, Pb, Li). The identities of essential elements are based on historical work and that done by Klaus Schwarz in the 1970s.¹ Other essential elements may be present in various biological species. Essentiality has been defined by certain

Table 1.1 Percentage Composition of Selected Elements in the Human Body

Element	Percentage (by weight)	Element	Percentage (by weight)
Oxygen	53.6	Silicon, Magnesium	0.04
Carbon	16.0	Iron, fluorine	0.005
Hydrogen	13.4	Zinc	0.003
Nitrogen	2.4	Copper, bromine	$2. \times 10^{-4}$
Sodium, potassium, sulfur	0.10	Selenium, manganese, arsenic, nickel	$2. \times 10^{-5}$
Chlorine	0.09	Lead, cobalt	$9. \times 10^{-6}$

Source: Adapted from reference 2.

criteria: (1) A physiological deficiency appears when the element is removed from the diet; (2) the deficiency is relieved by the addition of that element to the diet; and (3) a specific biological function is associated with the element.² Table 1.1 indicates the approximate percentages by weight of selected essential elements for an adult human.

Every essential element follows a dose–response curve, shown in Figure 1.1, as adapted from reference 2. At lowest dosages the organism does not survive, whereas in deficiency regions the organism exists with less than optimal function.

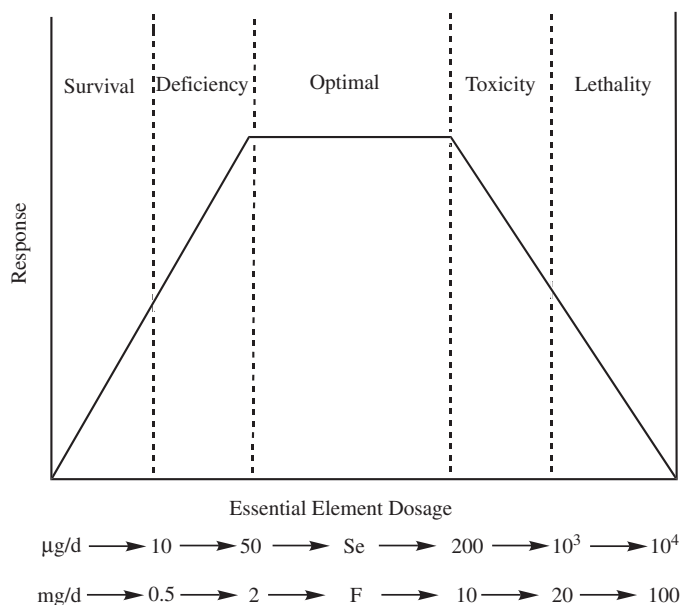


Figure 1.1 Dose–response curve for an essential element. (Adapted with permission from Figure 3 of Frieden, E. *J. Chem. Ed.*, 1985, **62**(11), 917–923. Copyright 1985, Division of Chemical Education, Inc.)

After the concentration plateau of the optimal dosage region, higher dosages cause toxic effects in the organism, eventually leading to lethality. Specific daily requirements of essential elements may range from microgram to gram quantities as shown for two representative elements in Figure 1.1.²

Considering the content of earth's contemporary waters and atmospheres, many questions arise as to the choice of essential elements at the time of life's origins 3.5 billion or more years ago. Certainly, sufficient quantities of the bulk elements were available in primordial oceans and at shorelines. However, the concentrations of essential trace metals in modern oceans may differ considerably from those found in prebiotic times. Iron's current approximate 10^{-4} mM concentration in sea water, for instance, may not reflect accurately its pre-life-forms availability. If one assumes a mostly reducing atmosphere contemporary with the beginnings of biological life, the availability of the more soluble iron(II) ion in primordial oceans must have been much higher. Thus the essentiality of iron(II) at a concentration of 0.02 mM in the blood plasma heme (hemoglobin) and muscle tissue heme (myoglobin) may be explained. Beside the availability factor, many chemical and physical properties of elements and their ions are responsible for their inclusion in biological systems. These include: ionic charge, ionic radius, ligand preferences, preferred coordination geometries, spin pairings, systemic kinetic control, and the chemical reactivity of the ions in solution. These factors are discussed in detail by Frausto da Silva and Williams.³

1.3 METALS IN BIOLOGICAL SYSTEMS: A SURVEY

Metals in biological systems function in a number of different ways. Group 1 and 2 metals operate as structural elements or in the maintenance of charge and osmotic balance (Table 1.2). Transition metal ions that exist in single oxidation states, such as zinc(II), function as structural elements in superoxide dismutase and zinc fingers, or, as an example from main group +2 ions, as triggers for protein activity—that is, calcium ions in calmodulin or troponin C (Table 1.3). Transition metals that exist in multiple oxidation states serve as electron carriers—that is, iron ions in cytochromes or in the iron–sulfur clusters of the enzyme nitrogenase or copper ions in

Table 1.2 Metals in Biological Systems: Charge Carriers

Metal	Coordination Number, Geometry	Preferred Ligands	Functions and Examples
Sodium, Na ⁺	6, octahedral	<i>O</i> -Ether, hydroxyl, carboxylate	Charge carrier, osmotic balance, nerve impulses
Potassium, K ⁺	6–8, flexible	<i>O</i> -Ether, hydroxyl, carboxylate	Charge carrier, osmotic balance, nerve impulses

Table 1.3 Metals in Biological Systems: Structural, Triggers

Metal	Coordination Number, Geometry	Preferred Ligands	Functions and Examples
Magnesium, Mg^{2+}	6, octahedral	<i>O</i> -Carboxylate, phosphate	Structure in hydrolases, isomerases, phosphate transfer, trigger reactions
Calcium, Ca^{2+}	6–8, flexible	<i>O</i> -Carboxylate, carbonyl, phosphate	Structure, charge carrier, phosphate transfer, trigger reactions
Zinc, Zn^{2+} (d^{10})	4, tetrahedral	<i>O</i> -Carboxylate, carbonyl, <i>S</i> -thiolate, <i>N</i> -imidazole	Structure in zinc fingers, gene regulation, anhydrases, dehydrogenases
Zinc, Zn^{2+} (d^{10})	5, square pyramid	<i>O</i> -Carboxylate, carbonyl, <i>N</i> -imidazole	Structure in hydrolases, peptidases
Manganese, Mn^{2+} (d^5)	6, octahedral	<i>O</i> -Carboxylate, phosphate, <i>N</i> -imidazole	Structure in oxidases, photosynthesis
Manganese, Mn^{3+} (d^4)	6, tetragonal	<i>O</i> -Carboxylate, phosphate, hydroxide	Structure in oxidases, photosynthesis

Table 1.4 Metals in Biological Systems: Electron Transfer

Metal	Coordination Number, Geometry	Preferred Ligands	Functions and Examples
Iron, Fe^{2+} (d^6)	4, tetrahedral	<i>S</i> -Thiolate	Electron transfer, nitrogen fixation in nitrogenases, electron transfer in oxidases
Iron, Fe^{2+} (d^6)	6, octahedral	<i>O</i> -Carboxylate, alkoxide, oxide, phenolate	
Iron, Fe^{3+} (d^5)	4, tetrahedral	<i>S</i> -Thiolate	Electron transfer, nitrogen fixation in nitrogenases, electron transfer in oxidases
Iron, Fe^{3+} (d^5)	6, octahedral	<i>O</i> -Carboxylate, alkoxide, oxide, phenolate	
Copper, Cu^+ (d^{10}), Cu^{2+} (d^9)	4, tetrahedral	<i>S</i> -Thiolate, thioether, <i>N</i> -imidazole	Electron transfer in Type I blue copper proteins

Table 1.5 Metals in Biological Systems: Dioxygen Transport

Metal	Coordination Number, Geometry	Preferred Ligands	Functions and Examples
Copper, Cu ²⁺ (<i>d</i> ⁹)	5, square pyramid 6, tetragonal	<i>O</i> -Carboxylate <i>N</i> -Imidazole	Type II copper oxidases, hydroxylases Type III copper hydroxylases, dioxygen transport in hemocyanin
Iron, Fe ²⁺ (<i>d</i> ⁶)	6, octahedral	<i>N</i> -Imidazole, porphyrin	Dioxygen transport in hemoglobin and myoglobin

azurin and plastocyanin (Table 1.4); as facilitators of oxygen transport—that is, iron ions in hemoglobin or copper ions in hemocyanin (Table 1.5); and as sites at which enzyme catalysis occurs—that is, copper ions in superoxide dismutase or iron and molybdenum ions in nitrogenase (Table 1.6). Metal ions may serve multiple functions, depending on their location within the biological system, so that the classifications in the Tables 1.2 to 1.6 are somewhat arbitrary and/or overlapping.^{4,5}

Table 1.6 Metals in Biological Systems: Enzyme Catalysis

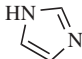
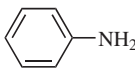
Metal	Coordination Number, Geometry	Preferred Ligands	Functions and Examples
Copper, Cu ²⁺ (<i>d</i> ⁹)	4, square planar	<i>O</i> -Carboxylate, <i>N</i> -imidazole	Type II copper in oxidases
Cobalt, Co ²⁺ (<i>d</i> ⁷)	4, tetrahedral	<i>S</i> -Thiolate, thioether, <i>N</i> -imidazole	Alkyl group transfer, oxidases
Cobalt, Co ³⁺ (<i>d</i> ⁶)	6, octahedral	<i>O</i> -Carboxylate, <i>N</i> -imidazole	Alkyl group transfer in vitamin B ₁₂ (cyanocobalamin)
Cobalt, Co ²⁺ (<i>d</i> ⁷)	6, octahedral	<i>O</i> -Carboxylate, <i>N</i> -imidazole	Alkyl group transfer in Vitamin B _{12r}
Cobalt, Co ⁺ (<i>d</i> ⁸)	6, octahedral, usually missing the 6th ligand	<i>O</i> -Carboxylate, <i>N</i> -imidazole	Alkyl group transfer in vitamin B _{12s}
Nickel, Ni ²⁺ (<i>d</i> ⁸)	4, square planar	<i>S</i> -Thiolate, thioether, <i>N</i> -imidazole, polypyrrrole	Hydrogenases, hydrolases
Nickel, Ni ²⁺ (<i>d</i> ⁸)	6, octahedral		Uncommon
Molybdenum, Mo ⁴⁺ (<i>d</i> ²), Mo ⁵⁺ (<i>d</i> ¹), Mo ⁶⁺ (<i>d</i> ⁰)	6, octahedral	<i>O</i> -Oxide, carboxylate, phenolate, <i>S</i> -sulfide, thiolate	Nitrogen fixation in nitrogenases, oxo transfer in oxidases

1.4 INORGANIC CHEMISTRY BASICS

Ligand preference and possible coordination geometries of the metal center are important bioinorganic principles. Metal ligand preference is closely related to the hard–soft acid–base nature of metals and their preferred ligands. These are listed in Table 1.7.⁶

In general, hard metal cations form their most stable compounds with hard ligands, whereas soft metal cations form their most stable compounds with soft ligands. Hard cations can be thought of as small dense cores of positive charge, whereas hard ligands are usually the small highly electronegative elements or ligand atoms within a hard polyatomic ion—that is, oxygen ligands in $(\text{RO})_2\text{PO}_2^-$ or in CH_3CO_2^- . Crown ethers are hard ligands that have cavities suitable for encapsulating hard metal ions. The [18]-crown-6 ether shown in Figure 1.2 with its 2.6- to 3.2-Å hole provides a good fit for the potassium ion, which has a radius of 2.88 Å.⁶

Table 1.7 Hard–Soft Acid–Base Classification of Metal Ions and Ligands

Metals, Ions, Molecules				Ligands	
HARD				HARD	
H^+	Mg^{2+}	Al^{3+}	SO_3	Oxygen ligands in H_2O , CO_3^{2-} , NO_3^- , PO_4^{3-} , ROPO_3^{2-} , $(\text{RO})_2\text{PO}_3^-$, CH_3COO^- , OH^- , RO^- , R_2O , and crown ethers Nitrogen ligands in NH_3 , N_2H_4 , RNH_2 , Cl^-	
Na^+	Ca^{2+}	Co^{3+}	CO_2		
K^+	Mn^{2+}	Cr^{3+}			
	VO^{2+}	Ga^{3+}			
		Fe^{3+}			
		Tl^{3+}			
		Ln^{3+}			
		MoO^{3+}			
INTERMEDIATE					INTERMEDIATE
Fe^{2+} , Ni^{2+} , Zn^{2+} , Co^{2+} , Cu^{2+} , Pb^{2+} , Sn^{2+} , Ru^{2+} , Au^{3+} , SO_2 , NO^+					Br^- , SO_3^{2-} , nitrogen ligands in NO_2^- , N_3^- , N_2
					
					
SOFT				SOFT	
Cu^+	Pt^{2+}	Pt^{4+}		Sulfur ligands in RSH , RS^- , R_2S , R_3P , RNC , CN^- , CO , R^- , H^- , I^- , $\text{S}_2\text{O}_3^{2-}$, $(\text{RS})_2\text{PO}_2^-$, $(\text{RO})_2\text{P}(\text{O})\text{S}^-$	
Au^+	Pb^{2+}				
Tl^+	Hg^{2+}				
Ag^+	Cd^{2+}				
Hg_2^{2+}	Pd^{2+}				

Source: Adapted from references 4 and 6.

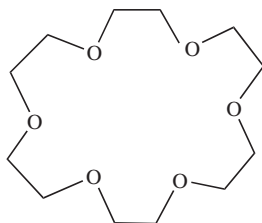


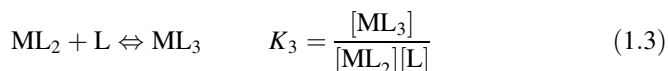
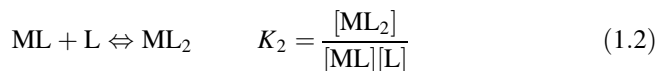
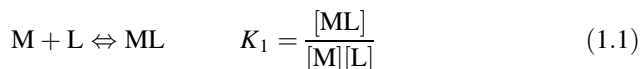
Figure 1.2 [18]-crown-6 ether.

It is possible to modify a hard nitrogen ligand toward an intermediate softness by increasing the polarizability of its substituents or the π electron cloud about it, an example being the imidazole nitrogen of the amino acid histidine. Increasing the softness of phosphate ion substituents can transform the hard oxygen ligand of $(RO)_2PO_2^-$ to a soft state in $(RS)_2PO_2^-$. Soft cations and anions are those with highly polarizable, large electron clouds—that is, Hg^{2+} , sulfur ligands as sulfides or thiolates, and iodide ions.

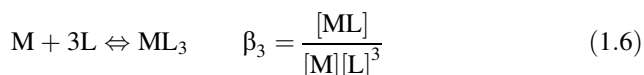
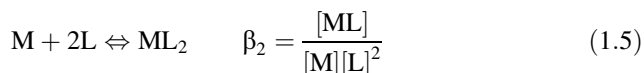
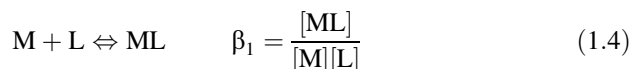
1.5 BIOLOGICAL METAL ION COMPLEXATION

1.5.1 Thermodynamics

The thermodynamic stability of metal ions are denoted by stepwise formation constants as shown in equations 1.1–1.3 (charges omitted for simplicity).



Alternately, they are indicated by overall stability constants as shown in equations 1.4–1.6:



The equation relating the stepwise and overall stability constants is indicated by equation 1.7:

$$\beta_n = K_1 K_2 \dots K_n \quad (1.7)$$

In biological systems, many factors affect metal–ligand complex formation. Hard–soft acid–base considerations have already been mentioned. Concentrations of the metal and ligand at the site of complexation are determined locally through concentration gradients, membrane permeability to metals and ligands, and other factors. Various competing equilibria—solubility products, complexation, and/or acid–base equilibrium constants—sometimes referred to as “metal ion speciation,” all affect complex formation. Ion size and charge, preferred metal coordination geometry, and ligand chelation effects all affect metal uptake. To better measure biological metal–ligand interactions, an “uptake factor” is defined as $K_{ML} \times [M]$, where K_{ML} is the stability constant K_1 and $[M]$ is the concentration of metal ion.³ Because naturally occurring aqueous systems have metal ion concentration varying roughly as

$$\begin{array}{ccccc} \text{K}^+, \text{Na}^+ & \text{Ca}^{2+}, \text{Mg}^{2+} & \text{Zn}^{2+} & \text{Cu}^{2+} & \text{Fe}^{2+} \\ 10^{-1} \text{ M} & \sim 10^{-3} \text{ M} & < 10^{-9} \text{ M} & < 10^{-12} \text{ M} & \sim 10^{-17} \text{ M} \end{array}$$

great selectivity for metal species is necessary to concentrate the necessary ions at sites where they are needed. Differentiating ligands are those preferred by the cation in question. A much more detailed discussion takes place in reference 3. Table 1.8 is adapted from this source.

1.5.2 Kinetics

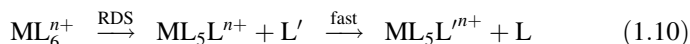
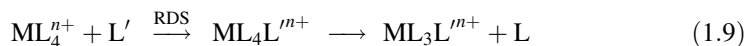
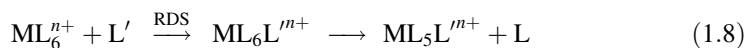
In biological systems, as in all others, metal ions exist in an inner coordination sphere, an ordered array of ligands binding directly to the metal. Surrounding this is

Table 1.8 K_{ML} and $K_{ML} \times [M]$ for Some Cations and Their Differentiating Ligands

	K^+, Na^+	$\text{Ca}^{2+}, \text{Mg}^{2+}$	$\text{Zn}^{2+}, \text{Cu}^{2+}$	Differentiating Ligand
K^+, Na^+				<i>O</i> -Macrocycles such as crown ethers, cryptates, and naturally occurring macrocyclic antibiotics such as nonactin and valinomycin
K_{ML}	>10	<10 ²	<10 ⁶	
$K_{ML} \times [M]$	>1.0	<0.1	<0.1	
$\text{Ca}^{2+}, \text{Mg}^{2+}$				Oxygen donors such as di- or tricarboxylates
K_{ML}	1.0	<10 ³	<10 ⁶	
$K_{ML} \times [M]$	<0.1	>1.0	<0.1	
$\text{Zn}^{2+}, \text{Cu}^{2+}$				Nitrogen and sulfur ligands
K_{ML}	0.1	<10 ²	>10 ⁶	
$K_{ML} \times [M]$	<0.1	<0.1	>1.0	

Source: Adapted from reference 3.

the outer coordination sphere consisting of other ligands, counterions, and solvent molecules. In stoichiometric mechanisms where one can distinguish an intermediate, substitution within the metals inner coordination sphere may take place through an associative (A), S_N2 process as shown in equations 1.8 (for six-coordinate complexes) and 1.9 (for four-coordinate complexes) or a dissociative (D), S_N1 mechanism as shown in equation 1.10 (RDS = rate determining step):



Associative mechanisms for metals in octahedral fields are difficult stereochemically (due to ligand crowding); therefore, they are rare for all but the largest metal ion centers. The associative mechanism is well known and preferred for four-coordinate square-planar complexes. Pure dissociative mechanisms are rare as well. When an intermediate cannot be detected by kinetic, stereochemical, or product distribution studies, the so-called interchange mechanisms (I) are invoked. Associative interchange (I_A) mechanisms have rates dependent on the nature of the entering group, whereas dissociative interchange (I_D) mechanisms do not.

The simplest reactions to study, those of coordination complexes with solvent, are used to classify metal ions as labile or inert. Factors affecting metal ion lability include size, charge, electron configuration, and coordination number. Solvents can be classified as to their size, polarity, and the nature of the donor atom. Using the water exchange reaction for the aqua ion $[\text{M}(\text{H}_2\text{O})_n]^{m+}$, metal ions are divided by Cotton, Wilkinson, and Gaus⁷ into four classes:

Class I. Rate constants for water exchange exceed 10^8 s^{-1} , essentially diffusion-controlled. These are classified as the labile species.

Class II. Rate constants for water exchange are in the range 10^4 – 10^8 s^{-1} .

Class III. Rate constants for water exchange are in the range 1 – 10^4 s^{-1} .

Class IV. Rate constants for water exchange are in the range 10^{-3} – 10^{-6} s^{-1} . These ions are classified as inert.

Labile species are usually main group metal ions with the exception of Cr^{2+} and Cu^{2+} , whose lability can be ascribed to Jahn–Teller effects. Transition metals of classes II and III are species with small ligand field stabilization energies, whereas the inert species have high ligand field stabilization energies (LFSE). Examples include Cr^{3+} ($3d^3$) and Co^{3+} ($3d^6$). Jahn–Teller effects and LFSE are discussed in Section 1.6. Table 1.9 reports rate constant values for some aqueous solvent exchange reactions.⁸

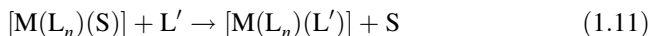
Outer-sphere (OS) reaction rates and rate laws can be defined for solvolysis of a given complex. Complex formation is defined as the reverse reaction—that is, replacement of solvent (S) by another ligand (L'). Following the arguments of

Table 1.9 Rate Constants for Water Exchange in Metal Aqua Ions

Class	Metal Ions	Rates log k (s ⁻¹)
I	Group IA (1), Group IIA (2) except Be and Mg, Group IIB (12) except Zn ²⁺ (3d ¹⁰), Cr ²⁺ (3d ⁴), Cu ²⁺ (3d ⁹)	8–9
II	Zn ²⁺ (3d ¹⁰)	7.6
	Mn ²⁺ (3d ⁵)	6.8
	Fe ²⁺ (3d ⁶)	6.3
	Co ²⁺ (3d ⁷)	5.7
	Ni ²⁺ (3d ⁸)	4.3
III	Ga ³⁺	3.0
	Be ²⁺	2.0
	V ²⁺ (3d ³)	2.0
	Al ³⁺	< 0.1
IV	Cr ³⁺ (3d ³), Co ³⁺ (3d ⁶), Rh ³⁺ (3d ⁶), Ir ³⁺ (3d ⁶), Pt ²⁺ (3d ⁸)	-3 to -6

Source: Adapted from references 7 and 8.

Tobe,⁹ in aqueous solution the general rate law for complex formation (eliminating charge for simplicity),



takes the second-order form shown in equation 1.12:

$$-d \frac{[\text{M}(\text{L}_n)(\text{S})]}{dt} = k' [\text{M}(\text{L}_n)(\text{S})] [\text{L}'] \quad (1.12)$$

The rate law frequently may be more complex and given as equation 1.13:

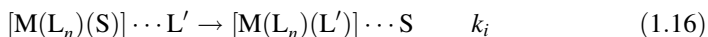
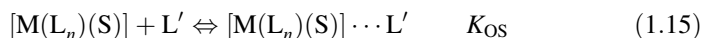
$$-d \frac{[\text{M}(\text{L}_n)(\text{S})]}{dt} = \frac{k'K [\text{M}(\text{L}_n)(\text{S})] [\text{L}']}{(1 + K[\text{L}'])} \quad (1.13)$$

Equation 1.13 reduces to the second-order rate law, shown in equation 1.12, when $K[\text{L}'] \lll 1$ and to a first-order rate law, equation 1.14,

$$-d \frac{[\text{M}(\text{L}_n)(\text{S})]}{dt} = k' [\text{M}(\text{L}_n)(\text{S})] \quad (1.14)$$

when $K[\text{L}'] \gggg 1$.

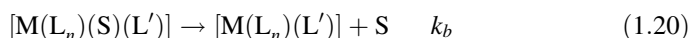
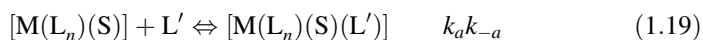
Interchange mechanisms (I_A or I_D) in a preformed OS complex will generate the following observed rate laws (which cannot distinguish I_A from I_D) with the equilibrium constant = K_{OS} (equation 1.15) and $k = k_i$ (equation 1.16):



The dissociative (D or S_N1) mechanism, for which the intermediate is long-lived enough to be detected, will yield equations 1.17 and 1.18, where $k = k_1$ and $K = k_2/(k_{-1}[S])$:



The associative (A or S_N2) will give the simple second-order rate law shown in equations 1.19 and 1.20 if the higher coordination number intermediate concentration remains small, resulting in the rate dependence shown in equation 1.21.



$$\frac{d[M(L_n)(S)]}{dt} = \frac{k_a k_b}{k_{-a} + k_b} [M(L_n)(S)][L'] \quad (1.21)$$

In all cases the key to assigning mechanism is the ability to detect and measure the equilibrium constant K . The equilibrium constant K_{OS} can be estimated through the Fuoss–Eigen equation,¹⁰ as shown in equation 1.22. Usually, K_{OS} is ignored in the case of $L' = \text{solvent}$.

$$K_{OS} = \frac{4\pi N_A a^3}{3000} (e^{-V/kT}) \quad (1.22)$$

where a is the distance of closest approach of the oppositely charged ions ($\sim 5 \text{ \AA}$), N_A is Avogadro's number, and V is the electrostatic potential at that distance (equation 1.23).

$$V = \frac{Z_1 Z_2 e^2}{4\pi \epsilon_0 \epsilon_R a} \quad (1.23)$$

As the above discussion indicates, assigning mechanisms to simple anation reactions of transition metal complexes is not simple. The situation becomes even more difficult for a complex enzyme system containing a metal cofactor at an active site. Methods developed to study the kinetics of enzymatic reactions according to the Michaelis–Menten model will be discussed in Section 2.2.4.

1.6 ELECTRONIC AND GEOMETRIC STRUCTURES OF METALS IN BIOLOGICAL SYSTEMS

Tables 1.2–1.6 list some of the important geometries assumed by metal ions in biological systems. Common geometries adopted by transition metal ions that will

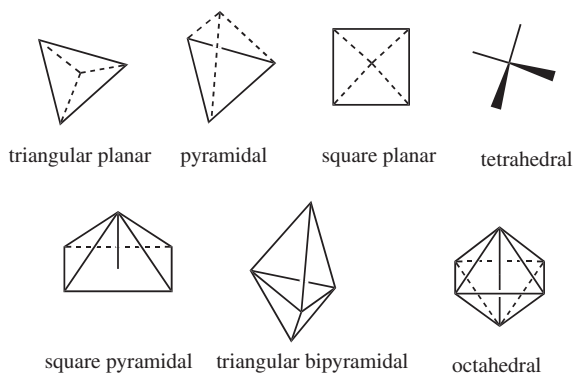


Figure 1.3 Common transition metal coordination geometries.

be of most concern to readers of this text are illustrated in Figure 1.3. In biological systems these geometries are usually distorted in both bond length and bond angle.

Transition metal ions play special roles in biological systems, with all elements from the first transition series except titanium (Ti) and scandium (Sc) occurring with great variety in thousands of diverse metalloproteins. Metals determine the geometry of enzymatic active sites, act as centers for enzyme reactivity, and act as biological oxidation–reduction facilitators. Molybdenum (Mo) appears to be the only transition element in the second transition series with a similar role. Vanadium (V), technetium (Tc), platinum (Pt), ruthenium (Ru), and gold (Au) compounds, as well as gadolinium (Gd) and other lanthanide complexes, are extremely important in medicinal chemistry as will be discussed in Chapter 7. Tables 1.2–1.6 list the *d*-electron configuration for transition metal ions common to biological systems. To find the number of *d* electrons for any transition metal ion, the following is a useful formula:

Number of *d* electrons =

$$\begin{aligned} &\text{Atomic number for the element}(Z) - \text{oxidation state of the element's ion} \\ &\quad - Z \text{ for the preceding noble-gas element}^4 \end{aligned}$$

Examples:

$$\begin{aligned} \text{Fe(II):} & \quad 26 - 2 - 18 \text{ (argon)} = 6 \\ \text{Mo(V):} & \quad 42 - 5 - 36 \text{ (krypton)} = 1 \end{aligned}$$

As a consequence of their partially filled *d* orbitals, transition metals exhibit variable oxidation states and a rich variety of coordination geometries and ligand spheres. Although a free metal ion would exhibit degenerate *d*-electron energy levels, ligand field theory describes the observed splitting of these *d*-electrons for metal ions in various ligand environments. In all cases the amount of stabilization or destabilization of *d*-electron energy levels centers about the so-called barycenter of unsplit *d*-electron energy levels. The most important of these for bioinorganic

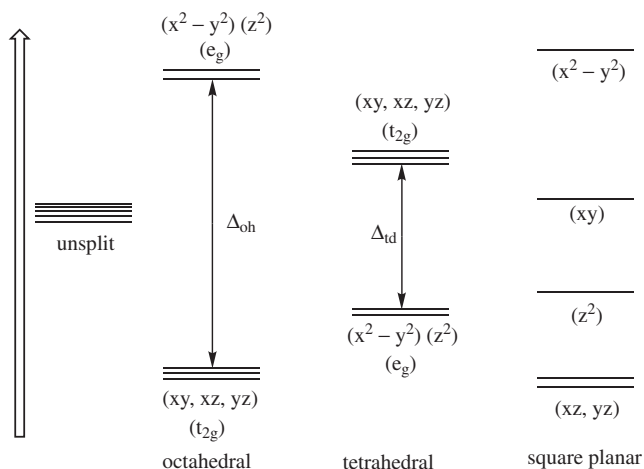


Figure 1.4 Approximate energy levels for d electrons in octahedral, tetrahedral, and square-planar fields.

applications are shown in Figure 1.4 for octahedral, tetrahedral, and square-planar ligand fields. The $t_{2g}(d_{xy}, d_{yz}, \text{ and } d_{xz})$ and $e_g(d_{x^2-y^2} \text{ and } d_{z^2})$ energy level designations identify symmetry properties of the d orbitals and are often used to indicate the degenerate energy levels under discussion. (See LFSE discussion below.) Generally, the energy gap for tetrahedral fields is approximately one-half that for octahedral fields, and that for square-planar fields is approximately $1.2\Delta_{\text{oh}}$. Many thermodynamic and kinetic properties of transition metal coordination complexes can be predicted by knowing the magnitude of Δ . Measurement of ultraviolet and visible absorption spectra of transition metal complexes that arise from these quantum mechanically forbidden $d-d$ transitions provide a measure of Δ .

To describe the d -orbital splitting effect for the octahedral field, one should imagine ligand spheres of electron density approaching along the x , y , and z axes, where the $d_{x^2-y^2}$ and d_{z^2} lobes of electron density point. Figure 1.5 illustrates representations of high-probability electron orbit surfaces for the five d orbitals.

For octahedral (O_h) geometry the repelling effect of like charge approach of the ligand electrons toward regions of high d electron density along the x , y , and z axes elevates the energy of the $e_g(d_{x^2-y^2} \text{ and } d_{z^2})$ orbitals while the $t_{2g}(d_{xy}, d_{yz}, \text{ and } d_{xz})$ orbitals are proportionally lowered in energy. For the tetrahedral (T_d) case, ligands approach between the x , y , and z axes, thereby stabilizing ($d_{x^2-y^2}$ and d_{z^2}) and destabilizing d_{xy} , d_{yz} , and d_{xz} orbital energy levels. For the square-planar case, ligands will approach along the x and y axes. Distorted octahedral and tetrahedral geometries are quite common in biological systems. Square-planar geometries, less common, are found for d^8 transition metal ions, especially for gold(III), iridium(I), palladium(II), and platinum(II) and for nickel(II) species in strong ligand fields. The platinum anticancer agent, *cis*-dichlorodiammineplatinum(II), shown in

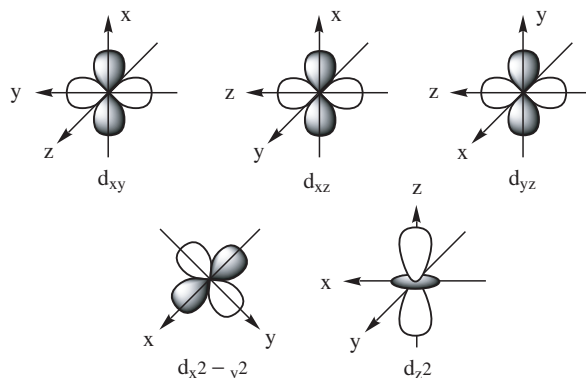


Figure 1.5 Representations of the five d orbitals along x , y , and z axes.

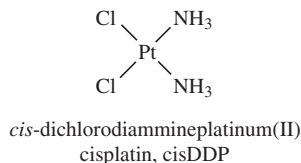
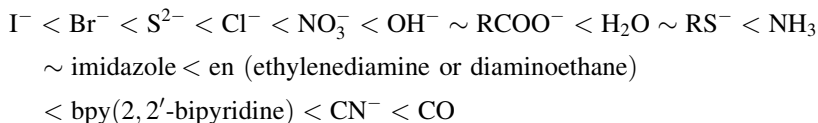


Figure 1.6 The antitumor active platinum compound *cis*-dichlorodiammineplatinum(II).

Figure 1.6, has a square-planar geometry all important for its utilization as an antitumor agent. See Section 7.2.3 for further discussion of this drug molecule.

The strength of the ligand field at a metal center is strongly dependent on the character of the ligand's electronic field and leads to the classification of ligands according to a "spectrochemical series" arranged below in order from weak field (halides, sulfides, hydroxides) to strong field (cyanide and carbon monoxide):



Ligand field strength may determine coordination geometry. For example, NiCl_4^{2-} occurs as a tetrahedral complex (small splitting—small Δ_{td}), whereas $\text{Ni}(\text{CN})_4^{2-}$ occurs in the square-planar geometry (large energy gap—large Δ_{sp}). In octahedral fields, ligand field strength can determine the magnetic properties of metal ions because for d^4 through d^7 electronic configurations both high-spin (maximum unpairing of electron spins) and low-spin (maximum pairing of electron spins) complexes are possible. Possible configurations are shown in Figure 1.7. In general, weak field ligands form high-spin complexes (small Δ_{oh}) and strong field ligands

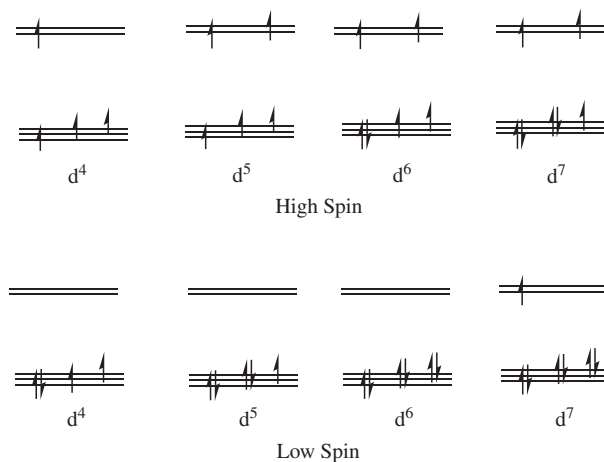


Figure 1.7 High-spin and low-spin d -electron configurations for the octahedral field.

form low-spin complexes (large Δ_{oh}). Detection of paramagnetism (unpaired electrons) and diamagnetism (all electrons paired) in bioinorganic ligand fields can help determine coordination geometry at active sites in enzymes. In the case of hemoglobin, for example, the d^6 iron(II) center cycles between high-spin and low-spin configurations affecting the placement of the iron center in or out of the plane of its porphyrin ligand. See Section 4.3 for further discussion. In Type III copper enzymes, two d^9 copper(II) centers become antiferromagnetically coupled resulting in a loss of the expected paramagnetism. See Sections 5.2.4 and 5.3.4.

The sum of the d -electron contributions to LFSE can be calculated with the formula shown in equation 1.24 for octahedral complexes:

$$\text{LFSE} = -\frac{2}{5}(\# e^- \text{ in } t_{2g})\Delta_{\text{oh}} + \frac{3}{5}(\# e^- \text{ in } e_g)\Delta_{\text{oh}} \quad (1.24)$$

where $\# e^-$ is the number of d electrons.

The $2/5$ stabilization (negative energy values) and $3/5$ destabilization (positive energy values) modifiers arise from the displacement of three d orbitals to lower energy versus two d orbitals to higher energy from the unsplit degenerate d -orbital state before imposition of the ligand field. Splitting values for d -orbital energy levels, based on $\Delta_{\text{oh}} = 10$, have been adapted from reference 7 and appear in Table 1.10.

The Jahn–Teller effect arises in cases where removal of degeneracy of a d -electron energy level is caused by partial occupation of a degenerate level. Two common examples are those of Cu(II) and Cr(II) as shown in Figure 1.8. Electrons in the e_g level could be placed in either the $d_{x^2-y^2}$ or d_{z^2} orbitals. Placing the odd electron in either orbital destroys the degeneracy of the e_g orbitals and usually has the effect of moving the ligands on one axis in or out. For Cu(II) complexes, this

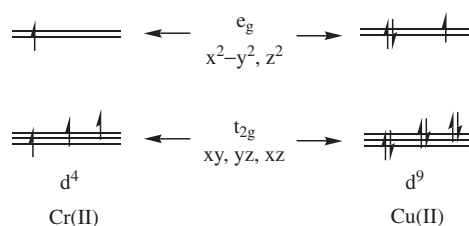
Table 1.10 Splitting Values for d Orbitals in Common Geometries

C. N. ^a	Geometry	$d_{x^2-y^2}$	d_{z^2}	d_{xy}	d_{xz}	d_{yz}
4	Tetrahedral	-2.67	-2.67	1.78	1.78	1.78
4	Square planar ^b	12.28	-4.28	2.28	-5.14	-5.14
5	Square pyramidal ^c	9.14	0.86	-0.86	-4.57	-4.57
6	Octahedral	6.00	6.00	-4.00	-4.00	-4.00

^aC. N. stands for coordination number.

^bBonds in xy plane.

^cPyramidal base in xy plane.

**Figure 1.8** Electron configurations for Cr(II) and Cu(II).

effect is very common, resulting in longer bond lengths on what is usually taken as the complex's z axis. The effect is also seen for high-spin d^4 Mn(III) and for low-spin d^7 Co(II) and Ni(III).

1.7 BIOORGANOMETALLIC CHEMISTRY

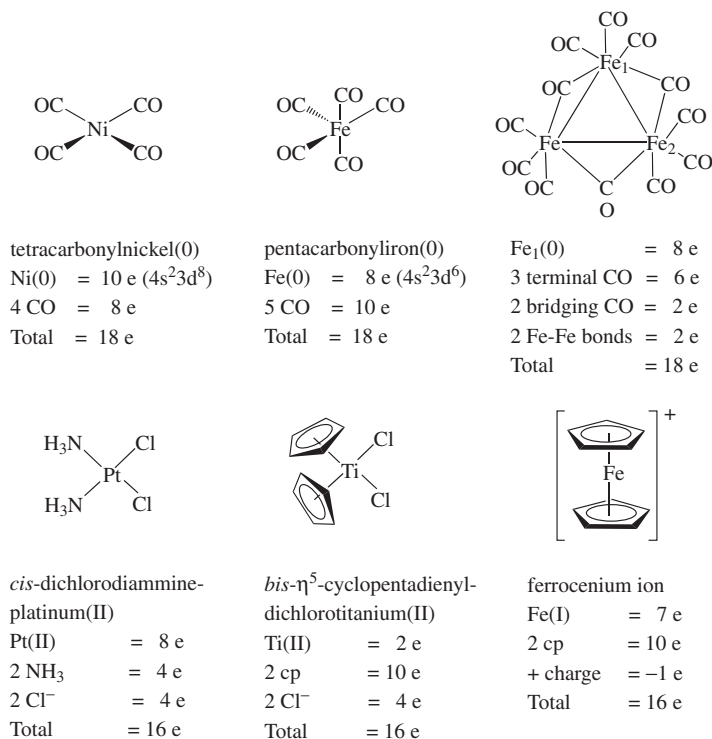
The eighteen (18-e) and sixteen (16-e) electron rules for organometallic complexes may also be applied to bioinorganic systems. In this system, the valence electrons of transition metals are considered to be filling the $4s$, $3d$, $4p$ or $5s$, $4d$, $5p$ shells. The most stabilized filled shell is determined to be eighteen electrons— s^2 , d^{10} , p^6 , differing by the 10 electrons of the filled d shell from main group element compounds stabilized by electron octets. Compounds or complexes fulfill the 18-e rule by addition of metal valence electrons and electron contributions from ligands. Metal valence shell electrons may be counted as if the metal, in its 0, +1, +2 oxidation states, combine with ligand electrons counted according to Table 1.11. Many stable coordination complexes can be counted as having 16 electrons (16-e rule), especially those having square planar geometry and those bonded to aromatic rings through their π electronic systems. Two of these complexes, belonging to a group of compounds called metallocenes, bind to DNA and are antitumor agents. The anticancer agent cisplatin, *cis*-dichlorodiammineplatinum(II), also obeys the 16-e rule. These complexes will be discussed in Chapter 7. Several illustrations of these molecules are shown in Figure 1.9.

Table 1.11 Ligand Contributions to the 18-Electron Rule

Ligand	Number of Electrons
Hydrogen H [•] , chloride radical Cl [•]	1
Alkyl or acyl groups	1
Carbonyl group	2
Nitrosyl group, linear	3
Lewis bases Cl ⁻ , O ²⁻ , S ²⁻ , NH ₃ , PR ₃	2
Alkenes	2 per double bond
Benzene	6 per ring (π donation)
cyclopentadienyl (cp) C ₅ H ₅ [•]	5 per ring

Many clusters contain metal–metal bonds, and these are counted by contributing one electron to each metal connected. Some simple examples in Figure 1.9 illustrate application of the rules.

Iron–sulfur clusters, such as those discussed in Chapter 6, cannot be treated using the 16-e or 18-e rules. Other frameworks exist to treat large metal clusters, and these have some utility in treating [Fe₄S₄]ⁿ⁺ clusters. One method treats the

**Figure 1.9** Molecules obeying the 16-e and 18-e rules.

number of metal atoms and the metal–metal bonds in a cluster according to the following formula¹¹:

$$\sum \text{Valence electrons} = \text{no. of cluster Me atoms} \\ \times 18 - \text{no. of metal-metal bonds} \times 2$$

Applying this formula to the cubane $[(\text{Fe}(\text{II}))_4(\eta^5\text{-C}_5\text{H}_5)_4(\mu_3\text{-S})_4]$ shown in Figure 1.10A results in the following electron count:

$$\sum \text{Valence electrons} = 4 \times 18 - 6 \times 2 = 60 \text{ electrons}$$

the so-called “magic number” for four metal atoms in a cluster.

If one applies the same procedure to Figure 1.10B, an iron–sulfur cluster often used as a model for those in biological systems, the same magic number of 60 would be obtained. Cluster magic numbers would occur as 48 e for a triangular clusters, 60 e for tetrahedral, 72 e for trigonal bipyramidal, 74 e for square pyramidal, 86 e for octahedral, 90 e for trigonal prisms, and 120 e for cubic structures.

For biological systems such as ferredoxins, problems arise when counting electrons by the valence electron method. This system assumes six Fe–Fe bonds within the tetrahedral iron–sulfur clusters, but Fe–Fe bond distances within biological iron sulfur clusters as found by X-ray crystallography do not often indicate Fe–Fe bonds. As discussed in reference 11, it is known that for the Fe_4S_4 cubane found in biological systems, oxidations are accompanied by increasing distortion of the cubane frame. Also, ^{57}Fe Mössbauer spectra indicate that the four iron atoms remain equivalent, suggesting delocalization within the Fe–S framework. Nitrogenase iron–sulfur clusters (discussed in Chapter 6) deviate substantially from the rules for $[\text{Fe}_4\text{S}_4]$ clusters discussed here.

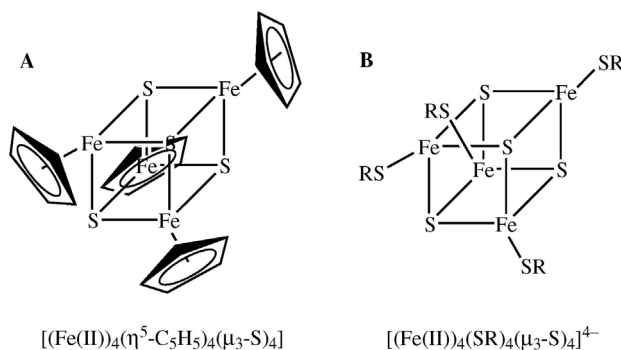
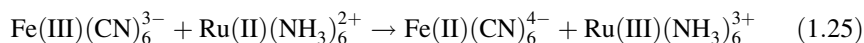


Figure 1.10 Cubanes (A) $[(\text{Fe}(\text{II}))_4(\eta^5\text{-C}_5\text{H}_5)_4(\mu_3\text{-S})_4]$ and (B) $[(\text{Fe}(\text{II}))_4(\text{SR})_4(\mu_3\text{-S})_4]^{4-}$.

1.8 ELECTRON TRANSFER

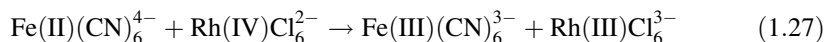
Many reactions catalyzed by metalloenzymes involve electron transfer. On the simplest level, one can consider electron transfer reactions to be complementary when there are equal numbers of oxidants and reductants and the metals transfer equal numbers of electrons as shown in equation 1.25:



Noncomplementary reactions, as shown in equation 1.26, involve unequal numbers of oxidants and reductants because the number of electrons gained or lost by each metal differs.⁶ Noncomplementary reactions, especially for large biomolecules, must proceed by a number of bimolecular steps because the possibility of termolecular or higher-order collisions is very small.



Two types of electron transfer mechanisms are defined for transition metal species. Outer-sphere electron transfer occurs when the outer, or solvent, coordination spheres of the metal centers is involved in transferring electrons. No reorganization of the inner coordination sphere of either reactant takes place during electron transfer. A reaction example is depicted in equation 1.27:



Inner-sphere electron transfers involve the inner coordination sphere of the metal complexes and usually take place through a bridging ligand. The classic example, typical of those studied and explained by H. Taube,¹² is illustrated by Figure 1.11's

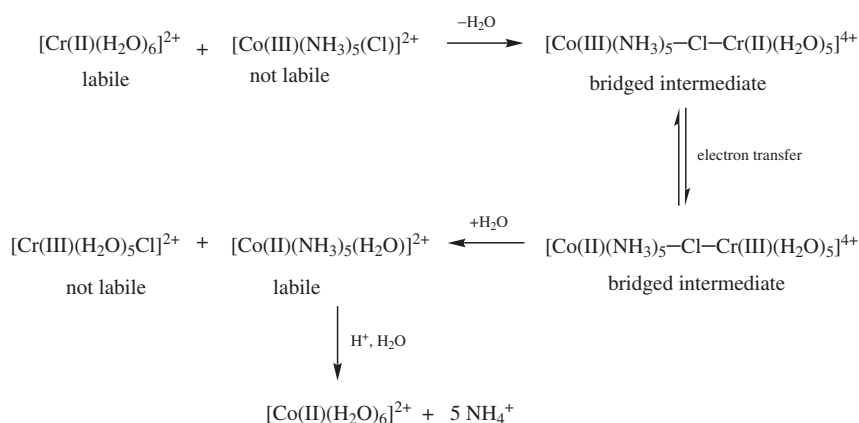


Figure 1.11 An inner-sphere electron transfer reaction sequence. (Adapted from reference 7.)

reaction sequence adapted from reference 7. In this reaction sequence, production of $[\text{Cr(III)}(\text{H}_2\text{O})_5\text{Cl}]^{2+}$ implies that electron transfer through the bridged intermediate from Cr(II) to Co(III) and Cl^- transfer from Co to Cr are mutually interdependent acts.

Harry B. Gray and Walther Ellis,¹³ writing in Chapter 6 of reference 13, describe three types of oxidation–reduction centers found in biological systems. The first of these, protein side chains, may undergo oxidation–reduction reactions such as the transformation of two cysteine residues to form the cystine dimer as shown in equation 1.28:



The second type of biological electron transfer involves a variety of small molecules, both organic and inorganic. Examples of these are (a) nicotinamide adenine dinucleotide (NAD) and nicotinamide adenine dinucleotide phosphate (NADP) as two electron carriers and (b) quinones and flavin mononucleotide (FMN), which may transfer one or two electrons. The structure of NAD and its reduced counterpart NADH are shown in Figure 1.12.

The third type of biological electron transfer involves metalloproteins themselves. These may be electron carriers (i.e., azurin) or proteins involved in the transport or activation of small molecules (i.e., nitrogenase). These so-called electron transferases have some or all of the following characteristics: (1) a suitable cofactor, such as NAD^+/NADH , acting as an electron source or sink; (2) geometry that allows the cofactor close enough to the protein surface for the transfer of electrons; (3) a hydrophobic shell on the protein surface around or near the cofactor; and (4) architecture that permits changes in protein conformation to facilitate electron transfer. These last changes should be small.¹⁴ Electron transferases that will be discussed in this text include the blue copper proteins such as azurin and plastocyanin (Chapter 5) and nitrogenase, one of the iron–sulfur proteins

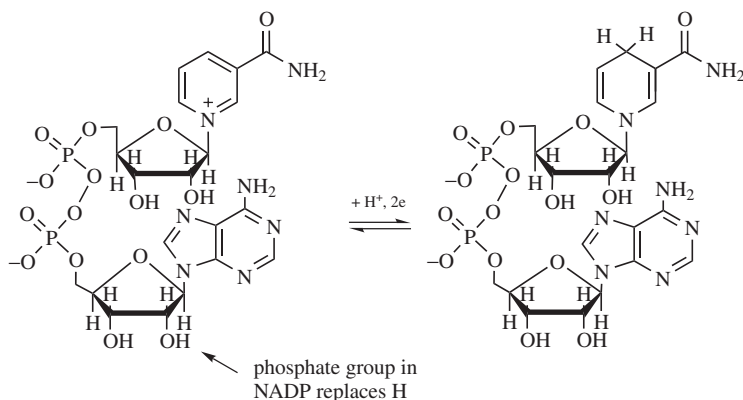
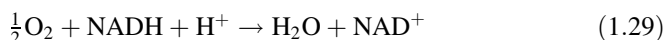


Figure 1.12 Electron transfer cofactors NAD^+ or NADH^+ .

(Chapter 6). Other iron–sulfur proteins, so named because they contain iron sulfur clusters of various sizes, include the rubredoxins and ferredoxins. Rubredoxins are found in anaerobic bacteria and contain iron ligated to four cysteine sulfurs. Ferredoxins are found in plant chloroplasts and mammalian tissue and contain spin-coupled [2Fe–2S] clusters. Cytochromes comprise several large classes of electron transfer metalloproteins widespread in nature. At least four cytochromes are involved in the mitochondrial electron transfer chain, which reduces oxygen to water according to equation 1.29. Further discussion of these proteins can be found in Chapters 6 and 7 of reference 13.



The simplest electron transfer reactions are outer sphere. The Franck–Condon principle states that during an electronic transition, electronic motion is so rapid that the metal nuclei, the metal ligands, and solvent molecules do not have time to move. In a self-exchange example,



the energies of donor and acceptor orbitals as well as bond lengths and bond angles remain the same during efficient electron transfer. In a cross reaction between two different species, one can write the following set of equilibrium statements (K) and rate equations (k_{et}):



Electron transfer theory is further explained by Marcus using potential energy diagrams to describe electron transfer processes.¹⁵ In the diagrams such as shown in Figure 1.13, electron donors and acceptors behave as collections of harmonic oscillators. The diagram expresses donor and acceptor in a single surface representing the precursor complex and one representing the successor complex. Point S represents the activated complex, and E_{R} and E_{P} are the reactant and product surfaces, respectively.

It is beyond the scope of this text to continue the discussion of Marcus theory. Qualitatively, the student should understand that electrons must find a path through the protein from the donor species to the acceptor. This may take place through bonds as outlined above or through electron tunneling events in which electrons travel through space between orbitals of the donor species to the acceptor species. Chapter 6 of reference 13 presents a clear explanation for further reading.

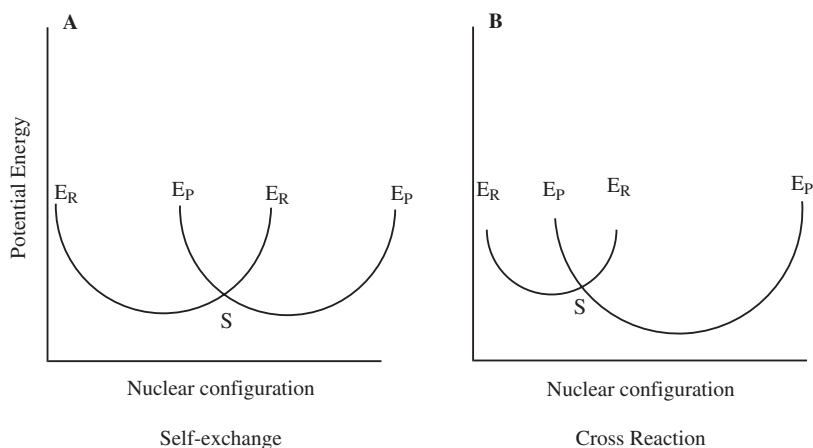


Figure 1.13 Potential energy diagrams describing electron transfer processes according to Marcus theory. (A) Self-exchange (B) Cross Reaction.

1.9 CONCLUSIONS

The preceding brief review of inorganic chemistry has been oriented toward questions that will arise in the following discussion of several bioinorganic systems. The inorganic and bioinorganic chemistry texts referenced in this chapter are good sources for answering the additional questions sure to arise in studying the behavior of metals in biological systems. It is important to keep in mind that metal behavior in the biological milieu will be influenced greatly by the surroundings. Metal-ligand systems existing in thermodynamic equilibrium and slow to react to changing cellular or noncellular dynamics will not long endure. Therefore, most of the metalloenzyme systems to be described in the following chapters contain metals in distorted and changeable ligand fields. These systems will continue to challenge the ingenuity of inorganic and bioinorganic chemists attempting to understand, modify, model, or design synthetic substitutes for them.

REFERENCES

1. Schwarz, K. *Ged. Proc.*, 1974, **33**, 1748–1757.
2. Frieden, E. *J. Chem. Ed.*, 1985, **62**(11), 917–923.
3. Frausto da Silva, J. J. R.; Williams, R. J. P. *The Biological Chemistry of the Elements: The Inorganic Chemistry of Life*, Clarendon Press, New York, 1991.
4. Lippard, S. J.; Berg, J. M. *Principles of Bioinorganic Chemistry*, University Science Books, Mill Valley, CA, 1994.

5. Hay, R. W. *Bio-Inorganic Chemistry*, Ellis Horwood Limited, Halsted Press, New York, 1984.
6. Cowan, J. A. *Inorganic Biochemistry, An Introduction*, 2nd ed., Wiley-VCH, New York, 1997.
7. Cotton, F. A.; Wilkinson, G.; Gaus, P. L. *Basic Inorganic Chemistry*, 3rd ed., John Wiley & Sons, New York, 1995, pp 192–194.
8. (a) Eigen, M. *Pure Appl. Chem.* 1963, **6**, 105. (b) Bennetto, H. P.; Caldin, E. F. *J. Chem. Soc. A*, 1971, 2198.
9. Tobe, M. L. Substitution Reactions, in *Comprehensive Coordination Chemistry*, Wilkinson, G., ed., Pergamon Press, Oxford, 1987, pp. 281–329.
10. Shriver, D. F.; Atkins, P. W.; Langford, C. H. *Inorganic Chemistry*, Oxford University Press, Oxford, 1990, pp. 477–478.
11. Elschenbroich, C. *Organometallics: A Concise Introduction*, VCH, New York, 1992.
12. Taube, H. *Electron Transfer Reactions of Complex Ions in Solution*, Academic Press, New York, 1970.
13. Gray, H. B.; Ellis, W. R., in Bertini, I.; Gray, H. B.; Lippard, S. J.; Valentine, J. S. *Bioinorganic Chemistry*, University Science Books, Mill Valley, CA, 1994, pp. 315–363.
14. Adman, E. T. *Biochim. Biophys. Acta*, 1979, **549**, 107–144.
15. Marcus, R. A. *Annu. Rev. Phys. Chem.*, 1964, **15**, 155–196.